Epithelial stem cell mutations that promote squamous cell carcinoma metastasis

Ruth A. White[1,2*], Jill M. Neiman[1*], Anand Reddi[1], Gangwen Han[1], Stanca Birlea[3], Doyel Mitra[1], Laikuan Dionne[1], Pam Fernandez[1], Kazutoshi Murao[3,4], Li Bian[1,5], Stephen B. Keysar[6], Nathaniel B. Goldstein[3], Ningjing Song[7], Sophia Bornstein[2], Zheyi Han[1], Xian Lu[8], Joshua Wisell[1], Fulun Li[1], John Song[9], Shi-Long Lu[4,9], Antonio Jimeno[4,6], Dennis R. Roop[3,4**], and Xiao-Jing Wang[1,3,4,9**]

Supplemental Data

Supplemental Materials and Methods

Human skin collection

Human skin punch biopsies (6 mm) were collected 24 hours after UV irradiation from 2 patients under the approval of Institutional Research Board of the University of Colorado Denver. Non–UV exposed skin was obtained from the National Disease Research Interchange (NDRI) from a healthy subject who underwent elective breast reduction surgery. The UV source was an Ultralite Phototherapy Chamber source (Narrow Band UVB Phototherapy Lamps 311 nm) (Ultralite Enterprises, Inc., Atlanta, GA); the dose given was 0.4 J/cm2. Shanghai Skin Diseases Hospital provided de-identified archived AK paraffin sections and approved the study as exempt for human subjects.

Genotyping

The K15.Kras^{G12D}.Smad4$^{f/f}$ mice were genotyped at 3 weeks of age. Tail snips were digested in proteinase K and DNA precipitated using ethanol. Genotyping was conducted by PCR

with primers that identify the presence of loxP sites in the transgene to differentiate between wild type and transgenic alleles as previously described (1).

Immunohistochemistry and immunofluorescence

Immunohistochemical staining was performed as previously described (2) using a Smad4 primary antibody (Santa Cruz Biotechnology Inc.) and counterstained with hematoxylin. Immunofluorescence staining was performed as previously described (2). Primary antibodies included E-Cadherin (1:200, eBioScience), α-catenin (1:200, Abcam), N-Cadherin (1:200, Abcam), vimentin (1:200, Sigma), Keratin 14 (1:200, Fitzgerald), Keratin 1 (Roop lab, 1:800), PCNA (sc-7907, 1:200, Santa Cruz), Keratin 15 (1:2,000; Covance), CPD (clone TDM-2; 1:4,000; Cosmo Bio), pH2AX (Ser139; clone 20E3; 1:100; Cell Signaling). Alexa Fluor 488-conjugated (green) or Alexa Fluor 594-conjugated (red) secondary antibodies (Invitrogen) were used for visualization.

Low density miRNA arrays

MicroRNA expression analysis was performed on TaqMan Low Density Rodent A v2.0 Arrays (Applied Biosystems) per the manufacturer's protocol. RNA from SP or $CD34^+/CD49f^+$ cells was isolated from primary and passaged tumors. Each array was run with RNA pooled from three tumors, and the arrays were run on three distinct RNA pools for each cell type. cDNA was prepared and amplified using paired pre-amplification kit and primers from Applied Biosystems. Array cards were run on an ABI 7900HT Fast qRT-PCR machine. Array qRT-PCR data was analyzed using a standard relative quantification (ΔΔCt) method. Relative quantification analysis between samples was performed using the RQ

Manager software from Applied Biosystems. The ubiquitously expressed mammalian U6 small RNA was used for normalization. Amplification curves of each miRNA represented on the plate were checked for adequate amplification. Assays that had Ct values greater than 32 cycles in all samples, or those that did not amplify, were considered to be not expressed or expressed at very low levels in the tumor samples.

Bioinformatics and selection of differentially expressed miRNAs

Bioinformatics analysis of the Taqman miRNA array data was conducted by the University of Colorado Denver Cancer Center Biostatistics Core using a false discovery rate (FDR) approach. For each comparison, a t-test was conducted on each of the $\Delta\Delta$Ct for the individual miRNAs on each array. Naïve p-values were ranked from lowest to highest and q value was calculated for each naïve p value defined as $q_1=335*p_1/1$, ..., $q_i=335*p_i/i$, etc. The minimum value in the series: q_i, q_{i+1},….,q_{335} was found and set as the FDR value for each miRNA. Samples were considered significant at an FDR<0.05. Given the small sample size, no miRNAs were found with an FDR<0.05. To identify miRNAs for further validation, those miRNAs with p values < 0.05 were chosen and ranked by relative fold change.

Generation of K15.Kras^{G12D}.Smad4-/- primary cell lines

Primary tumor cell cultures were generated as we previously described (3). Briefly, tumor pieces were digested in collagenase (Worthington) for 45 minutes at 37°C in 0.25% trypsin (Sigma) for 15 minutes at 37°C. Cells were filtered through a 40 μm filter and washed in DMEM with 10% FBS. Cells were plated in 10 cm culture dishes and cultured at 5% CO_2 in a standard cell culture incubator. Prior to subculturing, cells were treated with TrypLE (Life

Technologies) for 2 minutes and floating cells discarded to select for epithelial cells. This selection was repeated prior to the subsequent 3-5 subcultures or as needed to remove fibroblast contamination.

Luciferase Assays for miR-9 activity

Functional activity of miR-9 in vitro was carried out using a luciferase vector containing a miR-9 target sequence 3' to a luciferase gene as described (4). This pMIR-9-Luc reporter (Signosis) was transfected into cells with a Renilla control vector (pGL 4.74, Promega) using Lipofectamine 2000 as a transfection agent. After 48 hours cells were washed with PBS and lysed using Passive Lysis Buffer (Promega). Luciferase and Renilla absorbance were read using the Dual Luciferase Kit (Promega) per manufacturer's instructions.

In vitro proliferation assay and cell cycle analyses

In vitro cell proliferation was measured using a WST-8 [2-(2-methoxy-4-nitrophenyl)-3-(4-nitrophenyl)-5-(2, 4-disulfophenyl)-2H-tetrazolium, monosodium salt] Cell Count Reagent (Nacalai Tesque, Inc.). For the cell growth assay, 50 cells were plated in a series of 96 well plates in triplicate. The proportion of viable cells was measured at 24, 48, and 72 hours by adding 10 μl of WST-8 Cell Count Reagent to each well. The plates were incubated at 37°C in a standard tissue culture incubator for 2 hours and absorbance of the reaction was measured at 450 nm using a micro plate reader. At an absorbance of 450 nm the WST-8 reagent is proportional to the number of viable cells.

For cell cycle analysis, B911-GFP, B911-miR-9, B931-GFP and B931-Zip-9 cells were harvested and washed with PBS. Cells were stained with propidium iodide in 1 ml Krishan

Stain (5) at a concentration between 0.1-1x10^6 cells per ml at 4°C overnight. Cell cycle analysis was performed with a FC500 flow cytometer and data were analyzed using ModFit LT Software.

References

1. Bornstein, S., White, R., Malkoski, S., Oka, M., Han, G., Cleaver, T., Reh, D., Andersen, P., Gross, N., Olson, S., et al. 2009. Smad4 loss in mice causes spontaneous head and neck cancer with increased genomic instability and inflammation. *J Clin Invest* 119:3408-3419.
2. Lu, S.L., Herrington, H., Reh, D., Weber, S., Bornstein, S., Wang, D., Li, A.G., Tang, C.F., Siddiqui, Y., Nord, J., et al. 2006. Loss of transforming growth factor-beta type II receptor promotes metastatic head-and-neck squamous cell carcinoma. *Genes Dev* 20:1331-1342.
3. Go, C., He, W., Zhong, L., Li, P., Huang, J., Brinkley, B.R., and Wang, X.J. 2000. Aberrant cell cycle progression contributes to the early-stage accelerated carcinogenesis in transgenic epidermis expressing the dominant negative TGFbetaRII [In Process Citation]. *Oncogene* 19:3623-3631.
4. Acunzo, M., Visone, R., Romano, G., Veronese, A., Lovat, F., Palmieri, D., Bottoni, A., Garofalo, M., Gasparini, P., Condorelli, G., et al. 2012. miR-130a targets MET and induces TRAIL-sensitivity in NSCLC by downregulating miR-221 and 222. *Oncogene* 31:634-642.
5. Krishan, A. 1975. Rapid flow cytofluorometric analysis of mammalian cell cycle by propidium iodide staining. *J Cell Biol* 66:188-193.

Figure S1. DNA damaged cells in human bulge cells

(A) CPD and pH2AX staining showing that 24h after UV exposure in an Ultralite Phototherapy Chamber source (Narrow Band UVB Phototherapy Lamps 311 nm), CPD or pH2AX positive cells were mainly located in the interfollicular epidermis (green cells). Sporadic CPD or pH2AX positive cells are also seen in hair follicle cells, both $K15^{+}$ or $K15^{-}$ cells. Arrows point to CPD or pH2AX positive cells in K15+ cells. A non-UV exposed breast skin sample was used as a control. Scale bar=20 μm (B) CPD and pH2AX staining in biopsies of actinic keratosis (AK).. A few CPD positive cells were detected in the epidermis and hair follicles adjacent to the AK (arrows). Cells positive for pH2AX (green) were also detected in the epidermis and hair follicles (both K15+ and K15-). Arrows point to pH2AX/K15 double positive cells. Breast skin was used as a control. Scale bar=50 μm. Dotted lines highlight epidermal boundary. The bulge regions were also mapped by CD200 staining in consecutive sections (not shown).

Figure S2. Generation of K15.Kras^{G12D}.Smad4$^{-/-}$ transgenic mice, genotyping and confirming Smad4 deletion

(A) Schematic of the mating strategy to generate K15.Kras^{G12D}.Smad4$^{-/-}$ trigenic mice. (B) qRT-PCR analysis demonstrating Smad4 mRNA loss in K15.Kras^{G12D}.Smad4$^{-/-}$ tumors relative to K15.Kras^{G12D} benign papillomas (*p=0.05). The residual Smad4 mRNA level represents stromal Smad4 expression. (C) IHC demonstrating Smad4 protein loss in K15.Kras^{G12D}.Smad4$^{-/-}$ tumor epithelium compared to K15.Kras^{G12D} benign papillomas. The scale bar=50 μm for both panels. (D) Immunofluorescence staining of a K15.Kras^{G12D}

papilloma shows patchy $K15^+$ cells in the basal layer. Middle panel: $K15^+$ cells are largely overlapping with proliferating, $PCNA^+$ cells. Bottom panel: $K15^+$ cells are distinct from differentiated K1 expressing keratinocytes. Scale bar=50 μm for all panels.

Figure S3. Passaged K15.Kras^{G12D}.Smad4$^{-/-}$ tumors undergo EMT

Immunofluorescence staining of EMT markers shows a loss of E-cadherin and α-catenin but a gain of N-cadherin and vimentin in passaged tumors compared to K15.Kras^{G12D} papillomas or primary K15.Kras^{G12D}.Smad4$^{-/-}$ SCCs. The scale bar=30 μm for all panels.

Figure S4. SP sizes correlated with EMT

(A) SP^+ cells do not contain $CD34^+$ and $CD49f^+$ cells. (B) Examples of differences in SP sizes from SCC (left panels) and SPCC (right panels) and their corresponding SP sizes in bottom panels. Verapamil is used for SP specificity. The scale bar=50 μm for both panels. (C) Increased SP size in SPCC tumors. Black diamonds represent individual tumors and grey bars represent average SP size for tumor type. SP size was significantly increased ($p=0.003$) in the SPCCs compared to well-differentiated SCCs. (D) Increased SP size in passaged tumors compared to primary. * $p = 0.05$ (E) No difference in $SP^-/CD34^+/CD49^+$ size after passaging. Diamonds represent individual tumors, bars represent averages for each category.

Figure S5. Cluster analysis of miRNA expression in primary and passaged SP or $CD34^+/CD49f^+$ cells

The left panel shows a section of clustered miRNAs differentially expressed in SP cells from primary and passaged tumors. Primary and passaged SP cells cluster separately. The right panel shows miRNAs expressed in primary and passaged $CD34^+/CD49^+$ cells, which do not cluster separately. Yellow boxes represent miRNAs expressed at levels higher than the average of all expressed miRNAs, and blue boxes represent miRNAs expressed at levels lower than the average of all expressed miRNAs.

Figure S6. Stable miR-9 transfection or knockdown in cells derived from K15.Kras^{G12D}.Smad4$^{-/-}$ tumors

(A) miR-9 expression in two K15.Kras^{G12D}.Smad4$^{-/-}$ cell lines relative to wild type (WT) primary keratinocytes. *p=0.0003 compared to WT keratinocytes; #p=9x10^{-8} compared to WT keratinocytes (n=3/group). (B) Increased expression of mature miR-9 in a stably transduced K15.Kras^{G12D}.Smad4$^{-/-}$ cell line (B911) relative to GFP transduced control cells, measured by qRT-PCR (n=3/group). (C) Increased miR-9 activity repressing luciferase expression in the stably transduced B911 cell line (n=3/group, p=9x10^{-9}). Activity was measured using a luciferase construct containing a miR-9 target sequence 3' to the luciferase gene. (D) Abrogation of miR-9-mediated inhibition of luciferase expression in B931-Zip-9 cells (n=3/group, p=9x10^{-5}). (E) Increased mature miR-9 expression in stably transduced FaDu cell lines relative to GFP transduced FaDu cells, measured by qRT-PCR (n=3/group, *p=0.007). (F) Increased mature miR-9 expression in stably transduced Cal27 cell lines relative to GFP transduced controls (n=3/group, *p=2.5x10^{-7}).

Figure S7. Effects of miR-9 on cell growth and cell cycle inhibition

(A) miR-9 overexpression inhibits B911 tumor cell growth *in vitro*. Cell proliferation was measured using a WST-8 colorimetric assay (n=3/group). (B) miR-9 overexpression decreases the percentage of cells in S-phase compared to control in B911 mouse tumor cell lines ($p=2x10^{-4}$). (C) Knockdown of miR-9 in the B931 mouse tumor line increases the percentage of cells in S-phase (p=0.004). Each cell cycle assay was done in triplicate. (D) Matrigel invasion assays show increased invasion of B911-miR-9 cells compared to B911-GFP cells ($p=6x10^{-5}$). (F) Increased invasion of Cal27-miR-9 cells compared to GFP controls. *p=0.0005.

Figure S8. *In vivo* tumor growth rate is not affected by miR-9

miR-9 overexpression in (A) B911 tumor cells (B911-miR-9, n=3/group), (B) FaDu tumor cells (FaDu-miR-9, n=8/group), or (C) knockdown in B931 cells (B931-Zip-9) did not alter tumor growth in immunosuppressed athymic nude mice. 1,000 B911-GFP or B911-miR-9 cells, 2,500 B931-GFP (n=5) or B931-Zip-9 cells (n=6) were subcutaneously injected into athymic nude mice. 150,000 FaDu-GFP or FaDu-miR-9 cells were injected to the floor of the mouth. Tumor growth was measured weekly. Error bars represent standard deviation.

Figure S9. miR-9 overexpression does not restore E-cadherin expression, but causes SPCC tumor morphology

(A) Immunofluorescence staining showing that both B911-GFP and B911-miR-9 tumors express high levels of N-cadherin (Red) but do not express E-cadherin (Green). Knockdown of miR-9 in B931-Zip-9 tumors does not restore E-cadherin expression compared to B931-GFP controls. Scale bar = 50 μm. (B) H&E staining showing that miR-9 increased SPCC

formation in a tumor derived from B911-miR-9 cells. Conversely, B931-GFP cells formed SPCC, whereas a tumor derived from B931-Zip-9 cells reversed to a more epithelial morphology. Boxed area in each panel is magnified in lower pane. Scale bar=50 μm for upper panels.

Figure S10. Histogram of SP sorting showing SP expansion induced by miR-9 (A, B), which can be targeted to reduce metastasis by combined verapamil with chemotherapy in B911 cells (C)

(A) A representative histogram of SP sorting showing the SP population increased in a tumor derived from B911-miR-9 cells compared to tumors derived from B911-GFP control cells. (B) A typical histogram of SP sorting with a reduced SP population in a tumor derived from B931-Zip-9 cells compared to tumors derived from B931-GFP control cells. Verapamil is used to validate specificity of SP sorting (A) and (B). (C) Treatment of tumor bearing mice with a combination of docetaxel and verapamil significantly reduced lung metastasis from tumors generated by B911 cells compared to either docetaxel or verapamil alone.* p=0.02 compared to either docetaxel or verapamil.

Figure S1

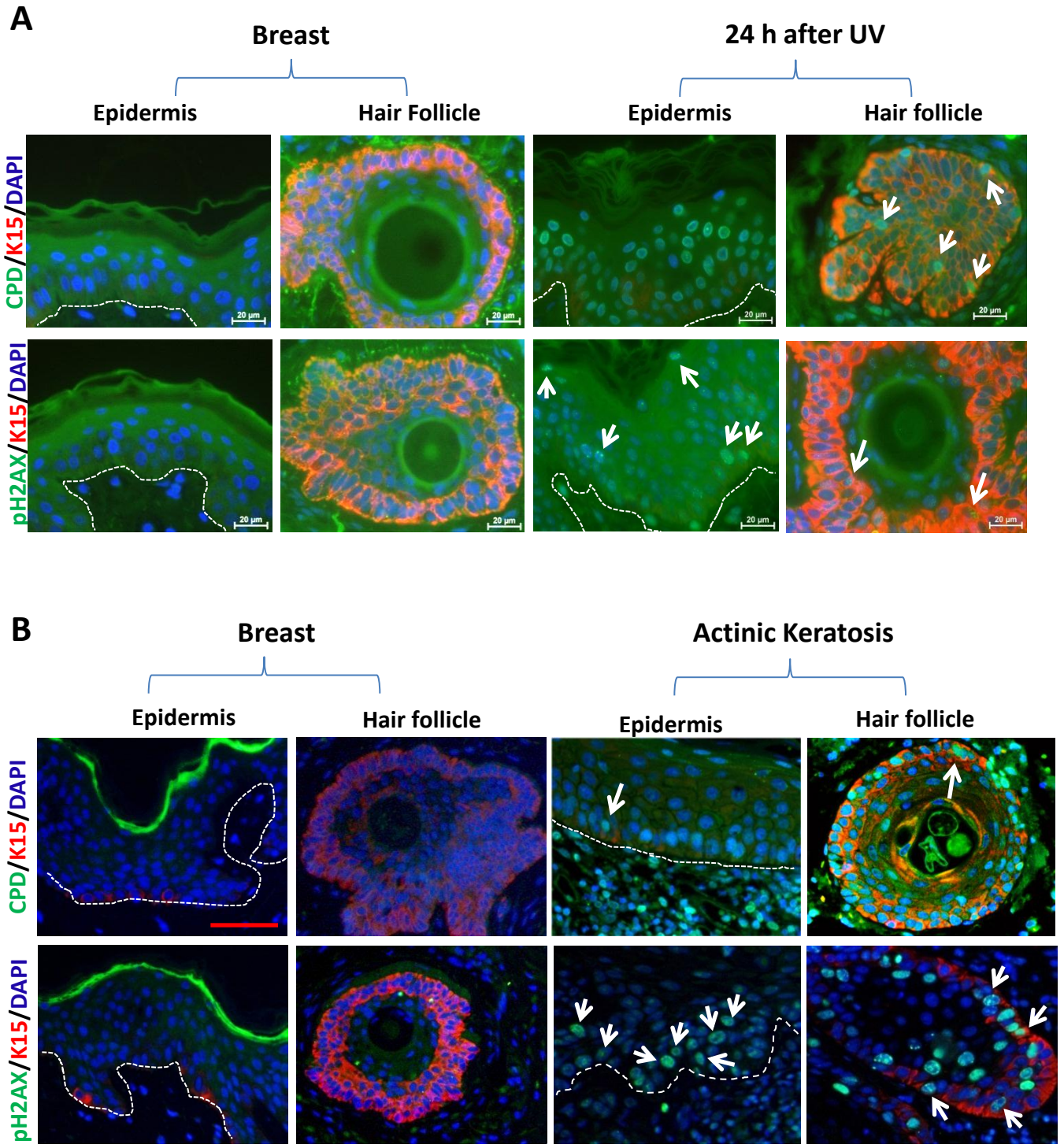
A
Breast
24 h after UV
Epidermis
Hair Follicle
Epidermis
Hair follicle
CPD/K15/DAPI
pH2AX/K15/DAPI
20 µm
B
Breast
Actinic Keratosis
Epidermis
Hair follicle
Epidermis
Hair follicle
CPD/K15/DAPI
pH2AX/K15/DAPI

Figure S2

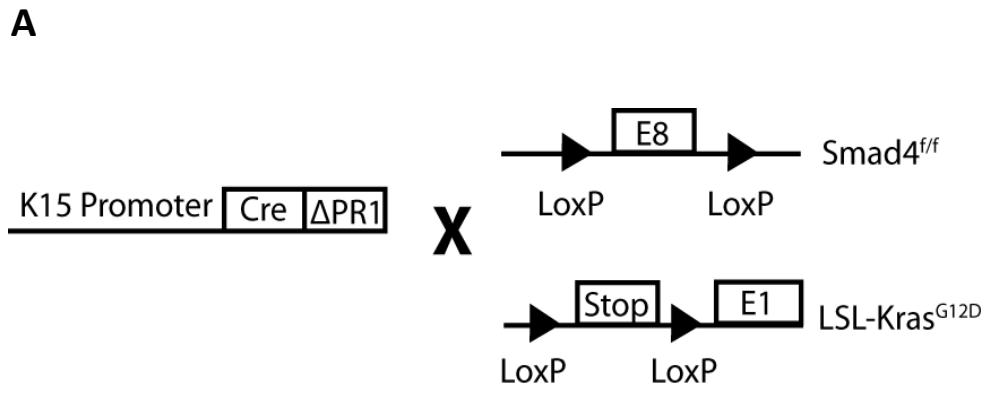
A
K15 Promoter
Cre
ΔPR1
X
E8
Smad4f/f
LoxP
LoxP
Stop
E1
LSL-KrasG12D
LoxP
LoxP

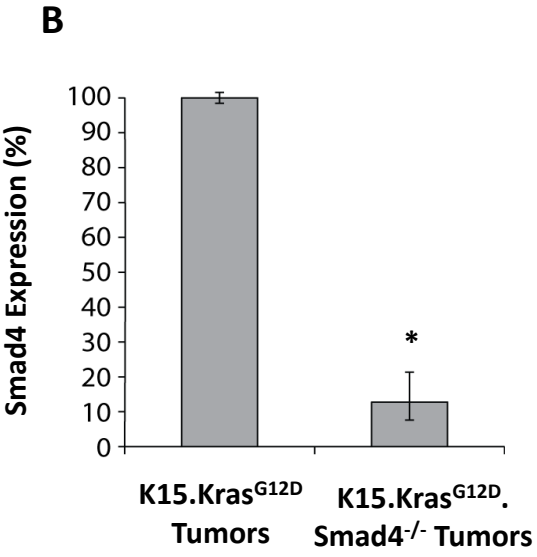
B
Smad4 Expression (%)
100
90
80
70
60
50
40
30
20
10
0
*
K15.KrasG12D Tumors
K15.KrasG12D. Smad4-/- Tumors

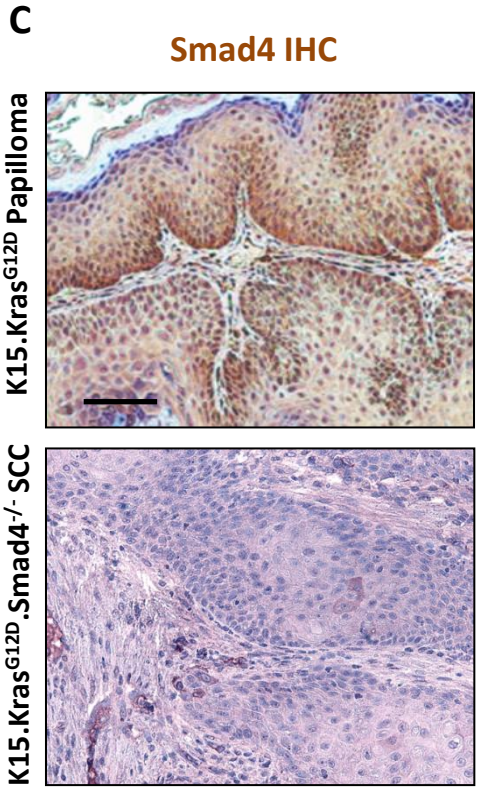
C
Smad4 IHC
K15.KrasG12D Papilloma
K15.KrasG12D.Smad4-/- SCC

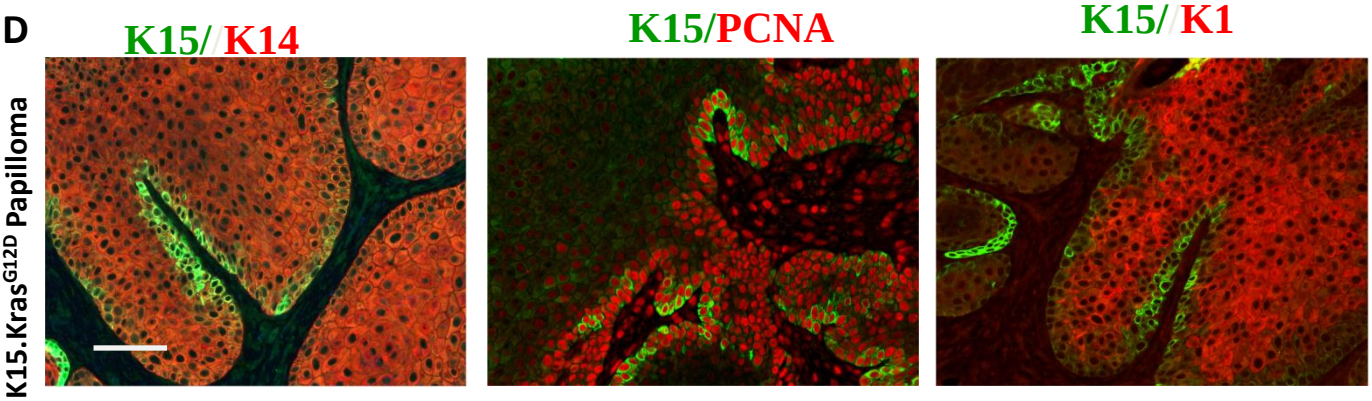
D
K15/ K14
K15/PCNA
K15/ K1
K15.KrasG12D Papilloma

Figure S3

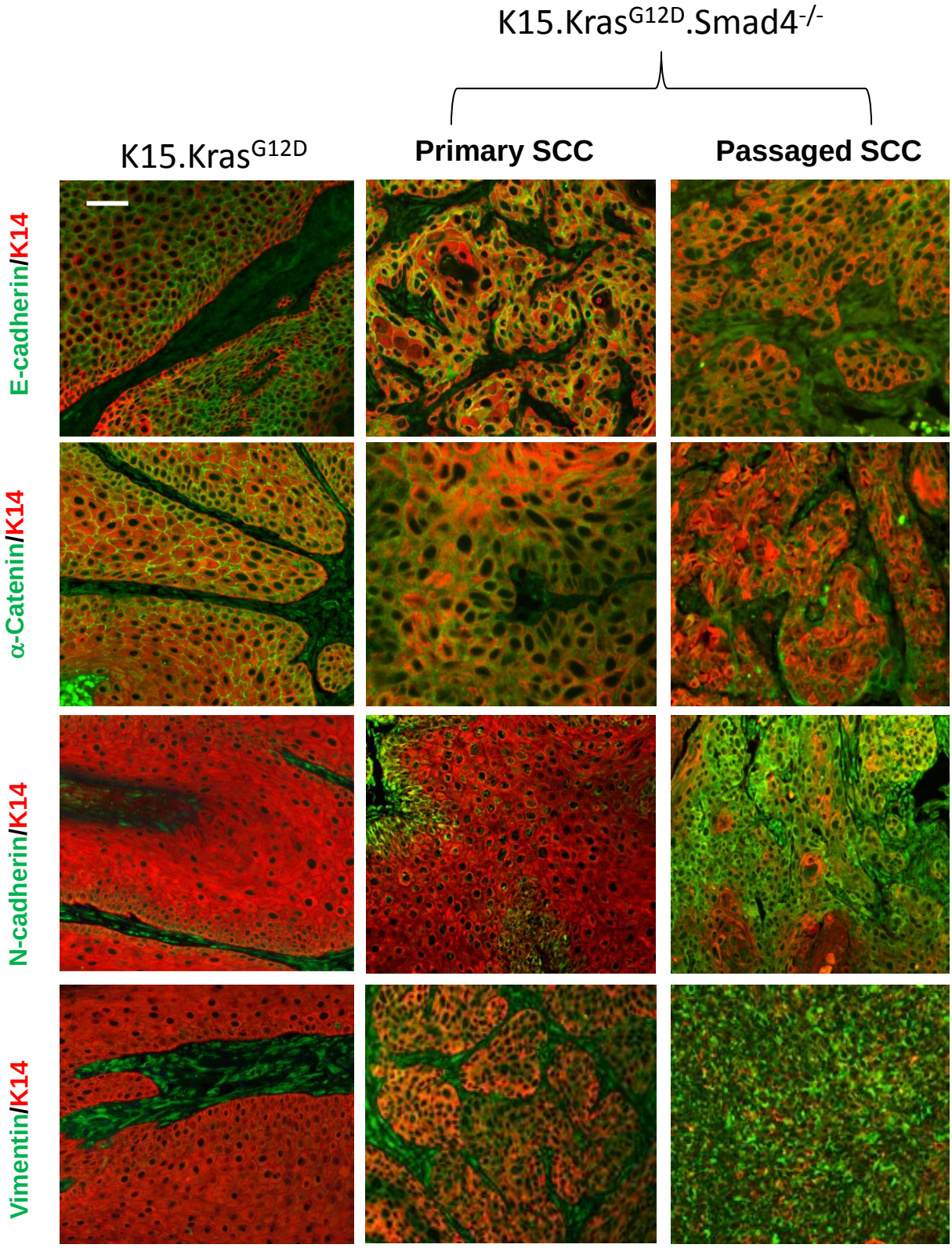
K15.Kras^{G12D}.Smad4$^{-/-}$
K15.Kras^{G12D}
Primary SCC
Passaged SCC
E-cadherin/K14
α-Catenin/K14
N-cadherin/K14
Vimentin/K14

Figure S4

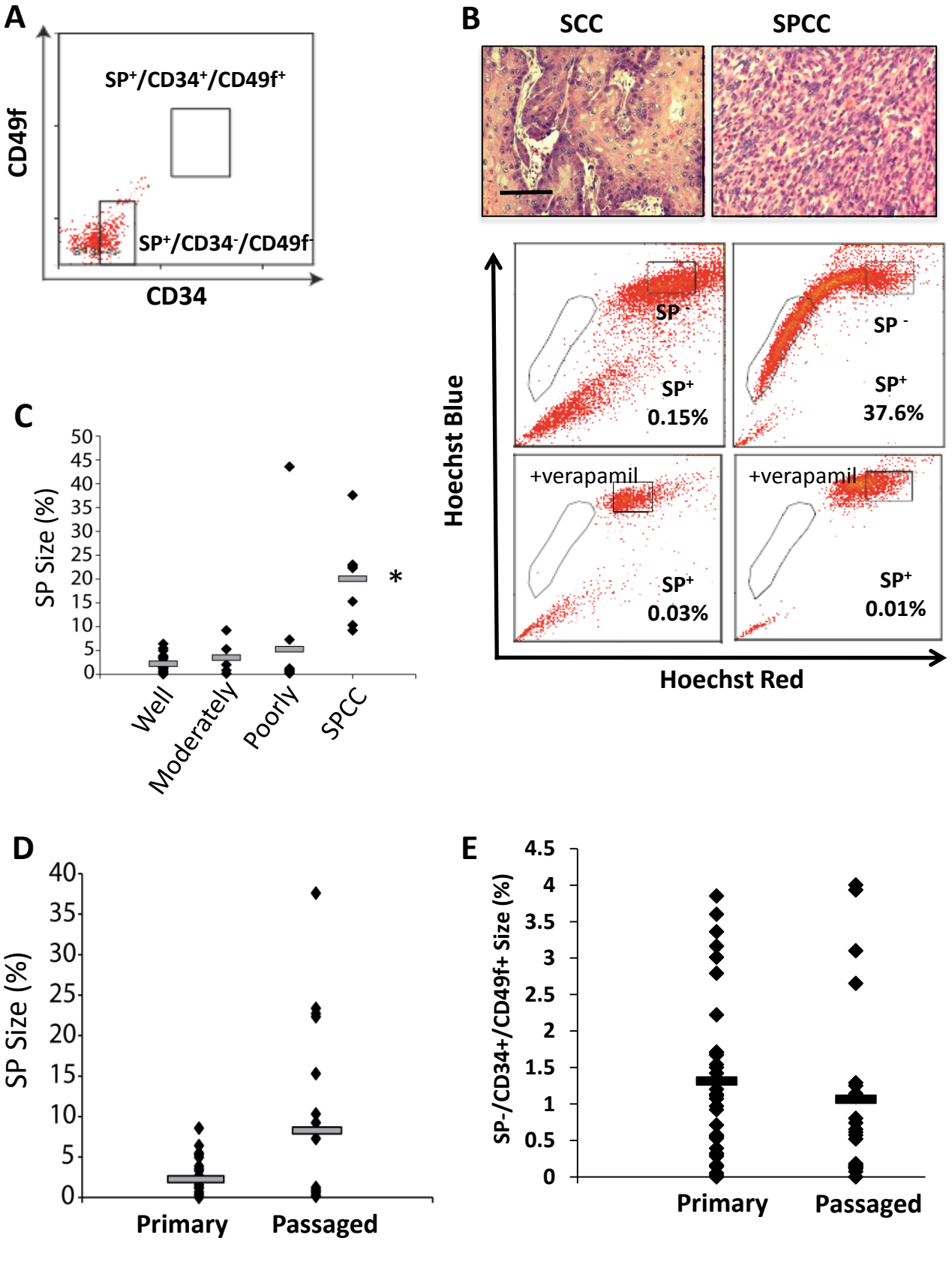
A
SP+/CD34+/CD49f+
SP+/CD34-/CD49f-
CD49f
CD34
B
SCC
SPCC
SP -
SP+
0.15%
SP -
SP+
37.6%
+verapamil
SP+
0.03%
+verapamil
SP+
0.01%
Hoechst Blue
Hoechst Red
C
SP Size (%)
50
45
40
35
30
25
20
15
10
5
0
*
Well
Moderately
Poorly
SPCC
D
SP Size (%)
40
35
30
25
20
15
10
5
0
Primary
Passaged
E
SP-/CD34+/CD49f+ Size (%)
4.5
4
3.5
3
2.5
2
1.5
1
0.5
0
Primary
Passaged

Figure S5

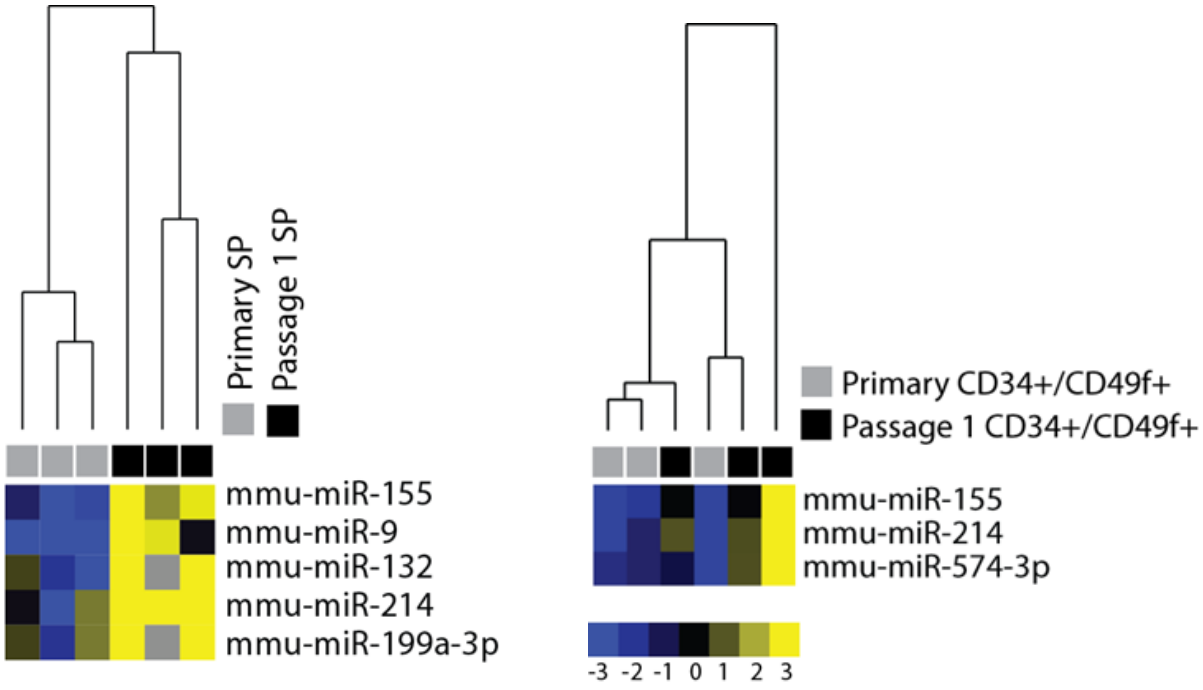
Primary SP
Passage 1 SP
mmu-miR-155
mmu-miR-9
mmu-miR-132
mmu-miR-214
mmu-miR-199a-3p
Primary CD34+/CD49f+
Passage 1 CD34+/CD49f+
mmu-miR-155
mmu-miR-214
mmu-miR-574-3p
-3 -2 -1 0 1 2 3

Figure S6

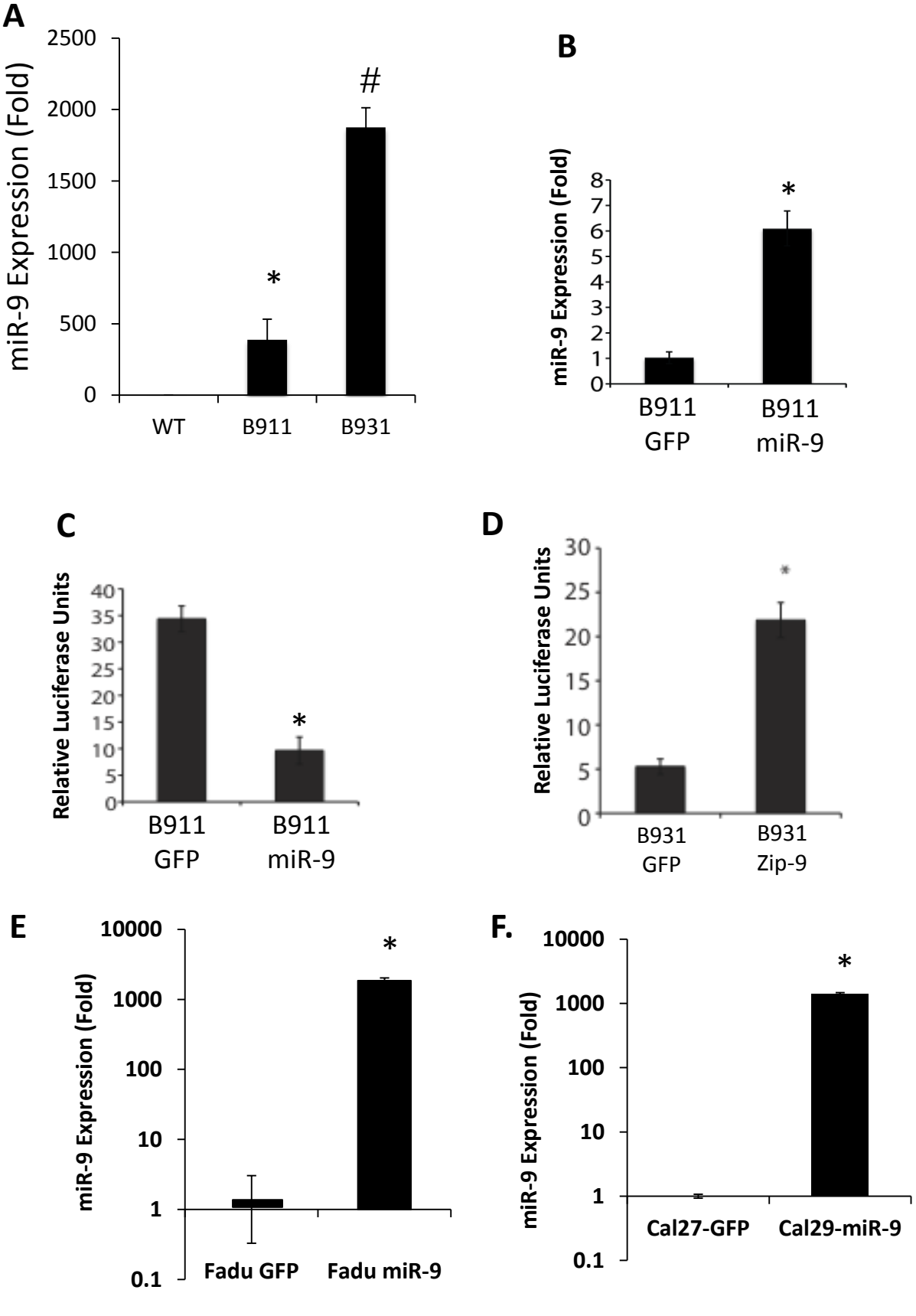
A
miR-9 Expression (Fold)
2500
2000
1500
1000
500
0
*
#
WT
B911
B931
B
miR-9 Expression (Fold)
8
7
6
5
4
3
2
1
0
*
B911 GFP
B911 miR-9
C
Relative Luciferase Units
40
35
30
25
20
15
10
5
0
*
B911 GFP
B911 miR-9
D
Relative Luciferase Units
30
25
20
15
10
5
0
*
B931 GFP
B931 Zip-9
E
miR-9 Expression (Fold)
10000
1000
100
10
1
0.1
*
Fadu GFP
Fadu miR-9
F.
miR-9 Expression (Fold)
10000
1000
100
10
1
0.1
*
Cal27-GFP
Cal29-miR-9

Figure S7

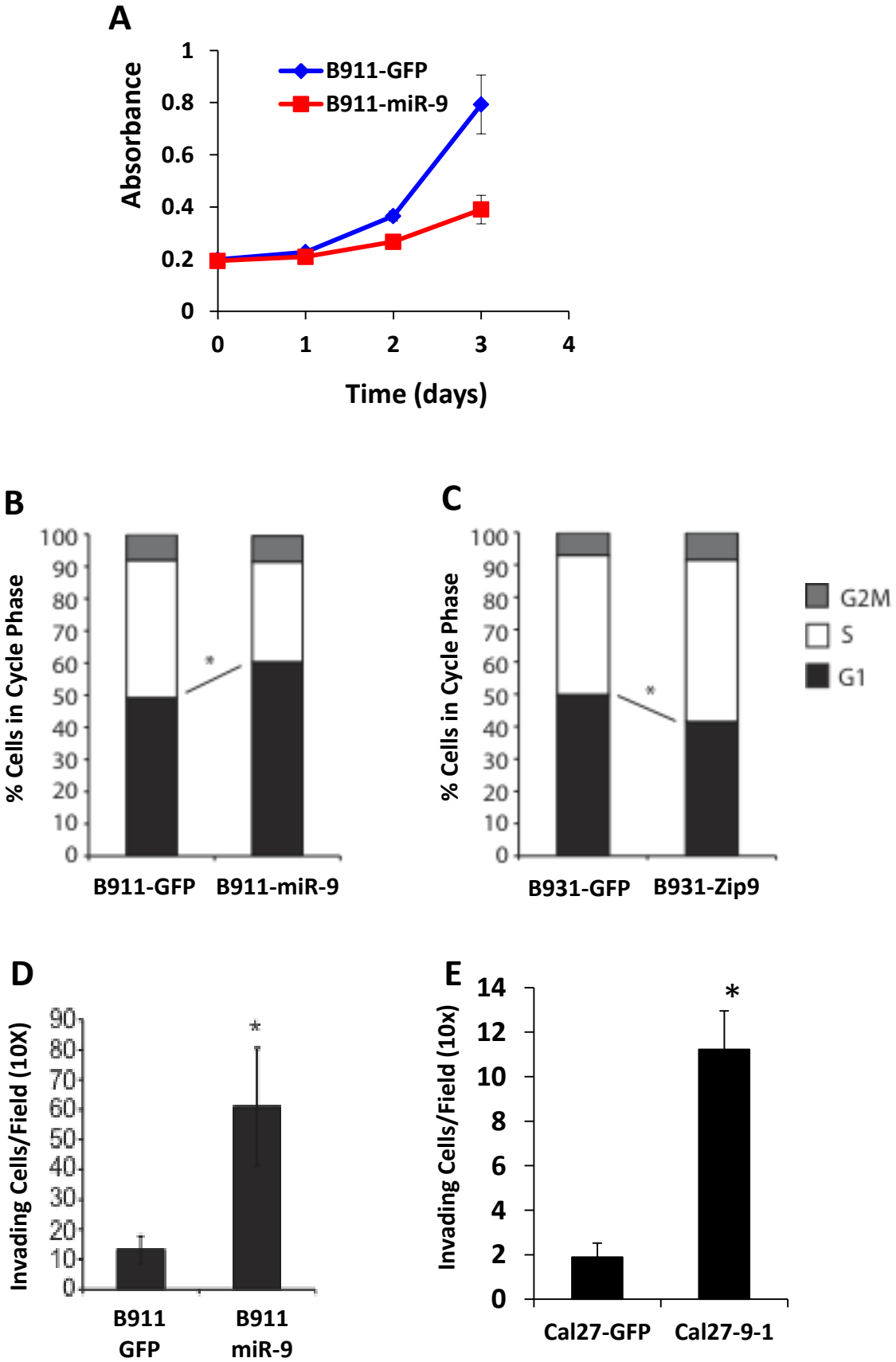
A
Absorbance
1
0.8
0.6
0.4
0.2
0
B911-GFP
B911-miR-9
0
1
2
3
4
Time (days)
B
% Cells in Cycle Phase
100
90
80
70
60
50
40
30
20
10
0
*
B911-GFP
B911-miR-9
C
% Cells in Cycle Phase
*
G2M
S
G1
B931-GFP
B931-Zip9
D
Invading Cells/Field (10X)
90
80
70
60
50
40
30
20
10
0
*
B911 GFP
B911 miR-9
E
Invading Cells/Field (10x)
14
12
10
8
6
4
2
0
*
Cal27-GFP
Cal27-9-1

Figure S8

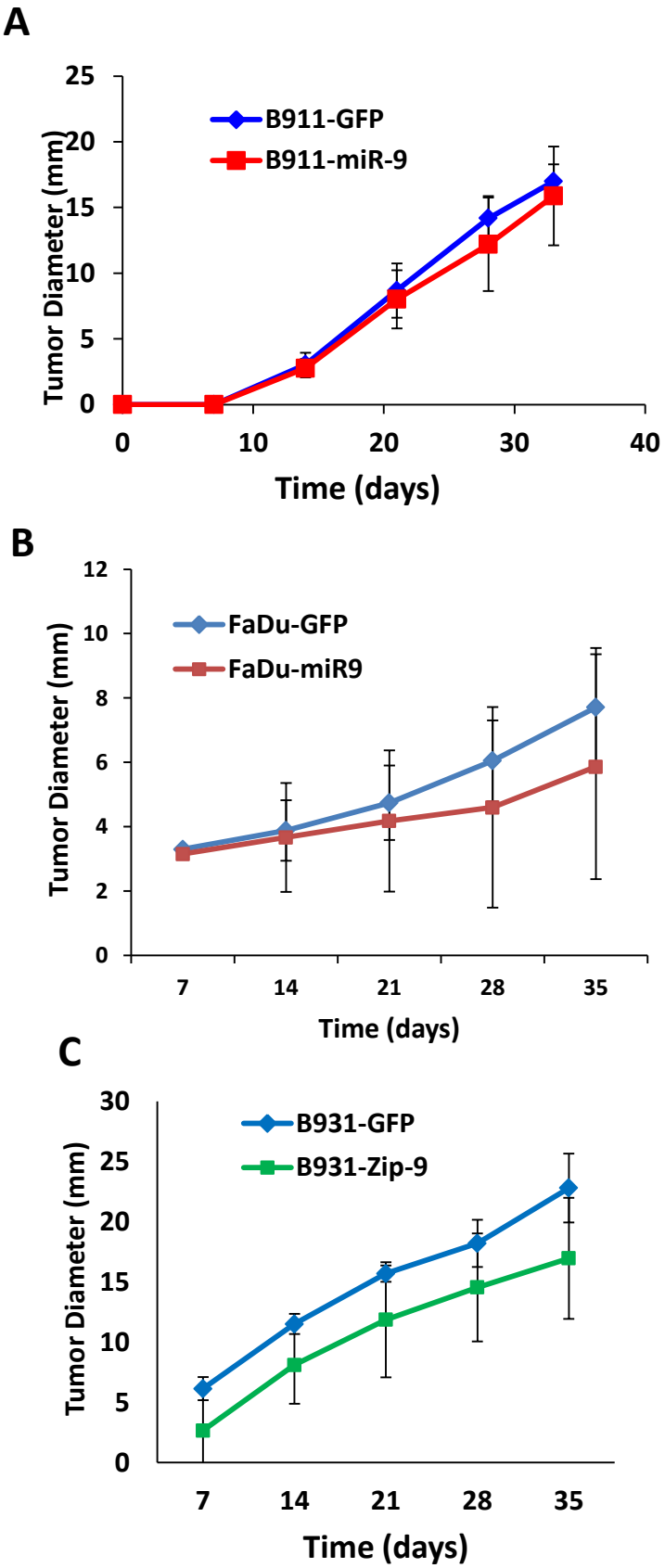
A
B911-GFP
B911-miR-9
Tumor Diameter (mm)
Time (days)
B
FaDu-GFP
FaDu-miR9
Tumor Diameter (mm)
Time (days)
C
B931-GFP
B931-Zip-9
Tumor Diameter (mm)
Time (days)

Figure S9

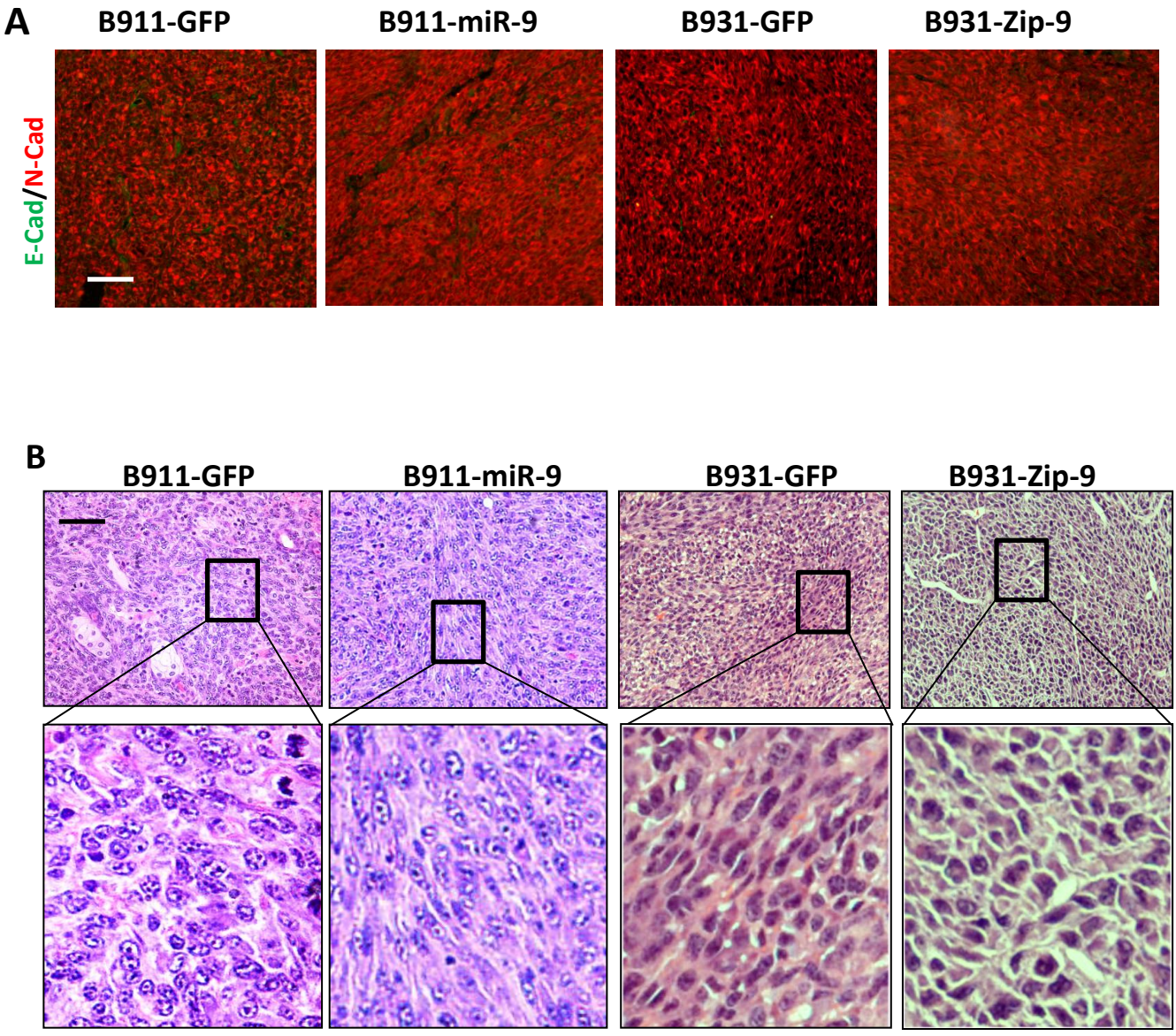
A
B911-GFP
B911-miR-9
B931-GFP
B931-Zip-9
E-Cad/N-Cad
B
B911-GFP
B911-miR-9
B931-GFP
B931-Zip-9

Figure S10

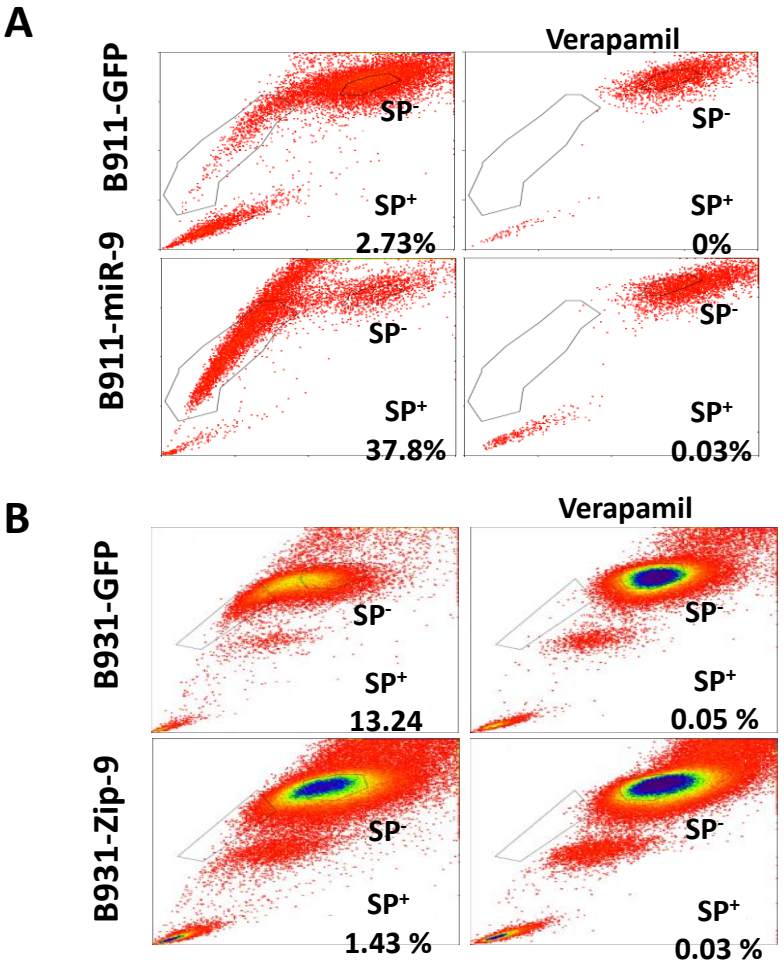
A
Verapamil
B911-GFP
B911-miR-9
SP-
SP+
2.73%
0%
37.8%
0.03%
B
Verapamil
B931-GFP
B931-Zip-9
SP-
SP+
13.24
0.05 %
1.43 %
0.03 %
C
B911
# of Visible Lung Metastasis
12
10
8
6
4
2
0
*
Docetaxel
Verapamil
Doc + Ver

Table S1 Summary of immunostaining markers in tumor samples

Genotype, Tumor type (n)	E-cadherin	α-catenin	N-cadherin	Vimentin	Keratin -1	Keratin-15
K15.Kras^{G12D} Papillomas (8)	8/8	8/8	2/8	1/8	8/8	8/8
K15.Kras^{G12D} .Smad4$^{-/-}$, Primary SCCs (10)	10/10	9/10	0/10	1/10	1/10 (p=0.0004)	10/10
K15.Kras^{G12D} .Smad4$^{-/-}$, Passaged SCCs (8)	1/8 (p=0.0003)	1/8 (p=0.003)	6/8 (p=0.0015)	6/8 (p=0.013)	0/8	2/8 (p=0.002)

Comparisons are made between primary and passages SCCs except keratin-1, which is compared between papillomas and primary SCCs. P values are calculated by Fisher's exact test

For Fig. 7B

B911

GFP miR-9

α-catenin

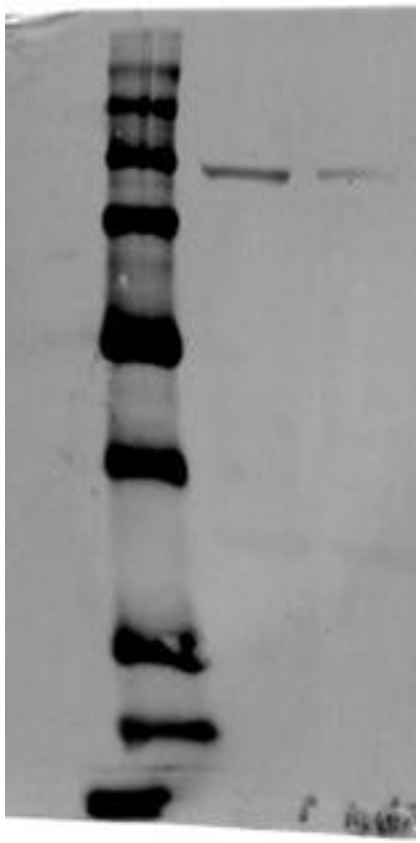

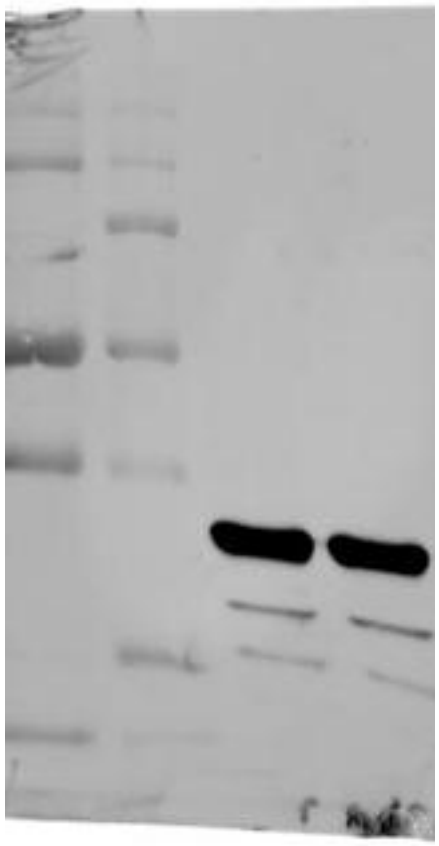

Gapdh, reprobe

For Fig. 7C

B931

GFP Zip-9

α-catenin

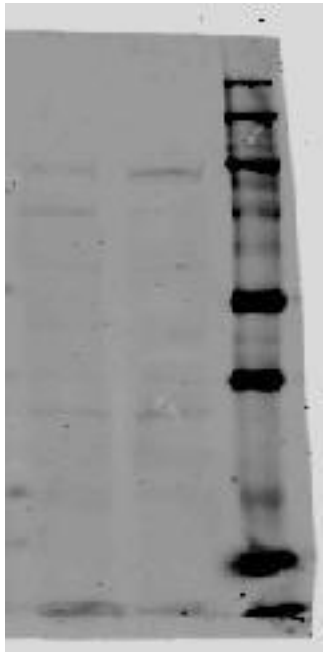

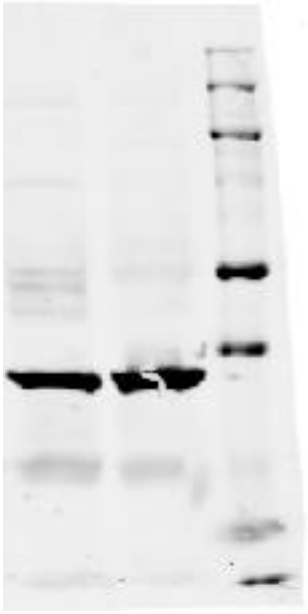

Gapdh, reprobe